

## Land-Cover Change Detection in Batur Catchment Area Using Remote Sensing

Ni Kadek Oki Febrianti<sup>1</sup>, Projo Danoedoro<sup>2</sup> , Prima Widayani<sup>3</sup> 

<sup>1</sup>Post-Graduated Student of Remote Sensing, Faculty of Geography, Gadjah Mada University, Indonesia

<sup>2,3</sup>Geographic Information Science Department, Faculty of Geography, Gadjah Mada University, Indonesia

### ARTICLE INFO

#### Article History:

Received: February 02, 2022

Revision: February 13, 2023

Accepted: February 15, 2023

#### Keywords:

Land-Cover Change

Batur

Catchment Area

Remote Sensing

#### Corresponding Author

E-mail:

kadekokifebrian@gmail.com

### ABSTRACT

Land cover information is an essential aspect in the planning and management of earth modeling and understanding. Land cover changes, such as hydrological conditions and ecological systems, impact the physical and social environment. This study aimed to identify spatial differences in the land cover of the Batur catchment area from 2015-2021 by using a remote sensing approach to describe the existing land-cover site and to detect its changes. The methods used in this study are a combination of the vegetation index and a supervised classification maximum likelihood algorithm with Landsat 8 OLI/TIRS in 2015 and 2021. Furthermore, the Change Detection Feature, identified from two image periods in 2015-2021 and processed, is used to detect changes in land cover. The accuracy assessment utilized QuickBird imagery recorded in 2015; field survey data were taken in 2021. The results showed that between 2015 to 2021, built-up area, bare land, shrubs, and lake have increased by 102,66% (306,01 ha), 27,95% (452,25 ha), 15,20% (215,72 ha) and 4,05 % (62,73 ha) while dryland forest and dry-dry-field have decreased by -25,84% (-606,29 ha) and -14,59% (-430,42 ha), respectively. The overall accuracy of the multispectral classification results in 2015 and 2021 was 82,63% and 89,57%.

### INTRODUCTION

One of the information needed for planning and management activities, and considered one important element in modeling and understanding the earth, is land-cover information (Lillesand et al., 2015). The land-cover type and its changes will impact the hydrology (Garg et al., 2019), soil erosion (Jazouli et al., 2019), climate (Sy & Quesada, 2020), and land surface temperature (Mukherjee & Singh, 2020). Land cover change is an important indicator for identifying the dynamics of land systems and the development of an environment (Abdullah et al., 2019). (Lin et al., 2020) state that continuous monitoring of land cover using satellite image classification helps regionalize land use policymaking.

Many studies have been carried out on land cover change, such as land cover

changes in Papua (Letsoin et al., 2020), identification of spatiotemporal pattern land use/land cover change under urbanization (Zhai et al., 2021), hydrological responses to land use/land cover change (Berihun et al., 2019). The denser the vegetation cover means less erosion and a less rate of soil loss (Tadele et al., 2017). (Berihun et al., 2019) states that land cover positively influences the annual surface runoff. The human factor is one of the factors that caused land cover change (Hua et al., 2015), processes of intensified anthropogenic accelerated land cover/land use change (Vinayak et al., 2021). Therefore, monitoring the land cover condition in an area, including the Batur catchment area, is crucial.

The identification of land-cover changes on a small scale can still be made manually in the field, but this is difficult to

do if changes occur on a large scale. Various efforts have been made to obtain the right method, one using a remote sensing approach. Remote sensing and system geographic information have been widely used to identify land cover change. Remote sensing offers the ability to measure land-cover change at different scales, locations, and times (Moser et al., 2013; Wu et al., 2017; Mohammadi et al., 2019). Multi-date remote sensing data images can provide information that can help classify the different component land use on a large scale at a lower cost (Barakat et al., 2019; Thyagarajan & Vignesh, 2019). One approach often used for land-cover identification is an image analysis approach based on digital classification (Rahman et al., 2012; Rwanga & Ndambuki, 2017; Sharma et al., 2017). The classification technique is pixel-based (Taati et al., 2016; Weih & Riggan, 2010), which aims to mark or label pixels in image data with information on earth (Aslami & Ghorbani, 2018). Supervised maximum likelihood is one multispectral classification commonly used for land-cover type (Rawat & Kumar, 2015; Bektas Balcik & Karakacan Kuzucu, 2016).

Recently, several researchers have focused on evaluating the potential of Landsat image data with various methods for classification, monitoring the land cover, and analyzing land-cover changes (Alkaradaghi et al., 2018; Phiri et al., 2018; Potapov et al., 2020). Landsat imagery is one of the optical images used in remote sensing for land-cover identification (Alam & Hossain, 2020; Mohamed et al., 2020; Rathnayake et al., 2020). Multi-temporal Landsat image data can detect land-cover change with medium resolution. Many researchers chose this image because it has been free since 2008 and can be accessed on the United States Geological Survey (USGS) website (Sun et al., 2018; Wulder et al., 2019).

The Batur catchment area is one of the catchment areas in Bali Province, with 101,62

km<sup>2</sup> area covering land and Lake Batur (P3E Bali Nusra, 2018). The Batur catchment area is at an altitude of 1,200 - 1,800 meters above sea level. The slope class of the Batur catchment area consists of a slope class of < 3% to >65%. Most low-slope slopes are located within the caldera area, while the relatively high slopes are on the edge of the caldera, and some are located on Mount Batur (P3E Bali Nusra, 2018). Soil physiography of the Batur catchment area is dominated by Caldera Valley and Volcanic Cone with 4,270.44 ha (42.02%) and 4,240.68 ha (41.72%). Meanwhile, the remaining 16% is the waters of Lake Batur, with an area of 1,651.32 ha (P3E, 2018).

Lake Batur is a closed caldera lake without an inlet and outlet (KLH, 2014). One problem of the Batur Catchment area disclosed in the 2014 GERMADAN document is land degradation of forest to non-forest lands such as agricultural land, settlements, and sand mining. The document also reveals the decrease in vegetation area due to land conversion resulting in high levels of erosion and sedimentation in the Lake Batur area (KLH, 2014).

The data shows that in 2014 the land conversion rate in the Batur Catchment area was quite high, such as decreased plantation area by 18,55% and forest by 11,98%. Conversely, the yard and agriculture food areas are increasing by 89,66 and 30,95% (KLH, 2014). This land conversion is feared to affect the condition of the lake waters. As stated by (Patil, 2018), changes in land usage as a consequence of human activities can disrupt the shape of the land surface and result in changes in the rate of erosion which most of the time occurs naturally. In 2015, Balai Wilayah Sungai (BWS), listed in 2018 in the Rencana Pengelolaan Sumber Daya Air dan Lahan (RPSDAL) document, stated there had been 5.980,74 m<sup>3</sup> sedimentation in Lake Batur. This sedimentation impacts

silting lake and decreases water volume by 47,2 million m<sup>3</sup> (P3E, 2018).

Using a remote sensing approach, this study aimed to identify spatial changes in land cover in the Batur catchment area in 2015-2021. We identified land-cover conditions in 2015 and 2021 and then compared and identified differences. This study uses a remote sensing approach to discuss spatial changes, so we do not specifically discuss the causes of changes outside of our system.

## RESEARCH METHODS

### Study Area

Batur catchment area is located between latitude 8°11'18,35"S and 8°17'35,45"S and longitude 115°19'16,42" E and 115°25'47,45"E Bangli District, Bali Province. Physiographically, the landscape of this area is mountainous in the form of a caldera bordered by circular hills around the caldera. Batur catchment areas are divided into six sub-catchments: Blingkang, Gede Tampuriang, Kedisan, Melilit, Serongga, and Trunyan (P3E, 2018). The study area is shown in Figure 1.

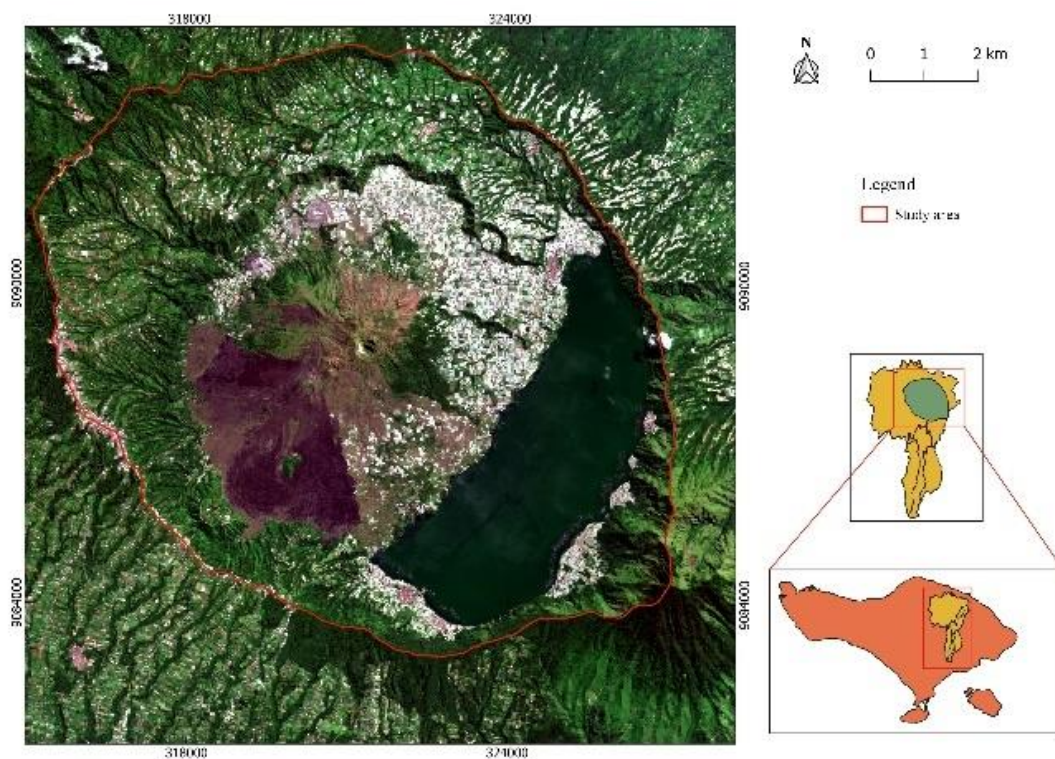


Figure 1. Study Area (Source: Sentinel 2-A, 2021)

### Processing and Analysis Stages

The stages of this research consist of (a) preparation and data acquisition, (b) image data preprocessing, (c) processing data consisting of composite bands and transforming vegetation index (NDVI), (d) taking training area (region of interest) (e) Multispectral classification of land-cover (f) field sampling (g) accuracy assessment of land-cover classification (h) detection of land-cover change. The details of the research flow chart are shown in Figure 2.

### Landsat Imagery, Spectral Indices, Classification, and Validation

This study used Landsat 8 OLI/TIRS multispectral imagery with a resolution of 30 meters spatial resolution consisting of 11 bands from coastal aerosol (band1) to thermal infrared (band 11). However, in this study, we only used bands 2 (blue), 3 (green), 4 (red), 5 (infrared), and 7 (swir 2). The explored datasets were Landsat OLI/TIRS C2 L2 path images 116 rows 066

captured on 17 May 2015 and 2 June 2021, QuickBird mosaic images captured in 2015 as accuracy testing material, shapefiles of 1:25,000 scale administrative boundaries from the Badan Informasi Geospasial (BIG), the boundary of Batur catchment area and the lake from Balai Wilayah Sungai (BWS) Bali Penida scale of 1:50.000.

The method used in this research was remote sensing. This study used the land-cover classification scheme of SNI 7645-1:2014. Land-cover analysis used a combination of vegetation index spectral transformations, namely the Normalized Difference Vegetation Index (NDVI) with supervised classification maximum likelihood. The emphasis was on land-cover conditions and identifying changes in two different study years, 2015 and 2021.

The formula of NDVI is shown in equation 1, where  $\rho_{NIR}$  and  $\rho_{RED}$  are radiometrically corrected, infrared band, and red band. NDVI is an index measuring the balance between the energy received and the energy emitted by an object on the ground (Nath, 2015). NDVI can be calculated by combining the red and NIR bands of the sensor system. The concept of NDVI technology is based on the principle that healthy vegetation has low visible

reflectance in the electromagnetic spectrum due to chlorophyll (Campbell, J.B., & Wynne, 2011).

$$NDVI = \frac{\rho_{NIR} - \rho_{RED}}{\rho_{NIR} + \rho_{RED}} \quad (1)$$

Maximum likelihood algorithms are one of the most common supervised classifications for processing sensor data (Anderson et al., 1976). This method assumes the probability that a pixel belongs to a particular class. These classes have equal probabilities, and the input bandwidth is considered to be normally distributed (Adebayo et al., 2019). Furthermore, accuracy assessment used the confusion matrix method, while the change detection utilized the change detection feature in ENVI software.

This research consisted of both in the field and remote sensing laboratory. We used a computer/ laptop for analysis and writing needs, ENVI software and Quantum GIS 3.16.14 for image data processing, Microsoft Office 2016 software for analysis and writing, Global Positioning System (GPS), and cameras for field survey needs. Other equipments for the field survey were a survey board and stationery.

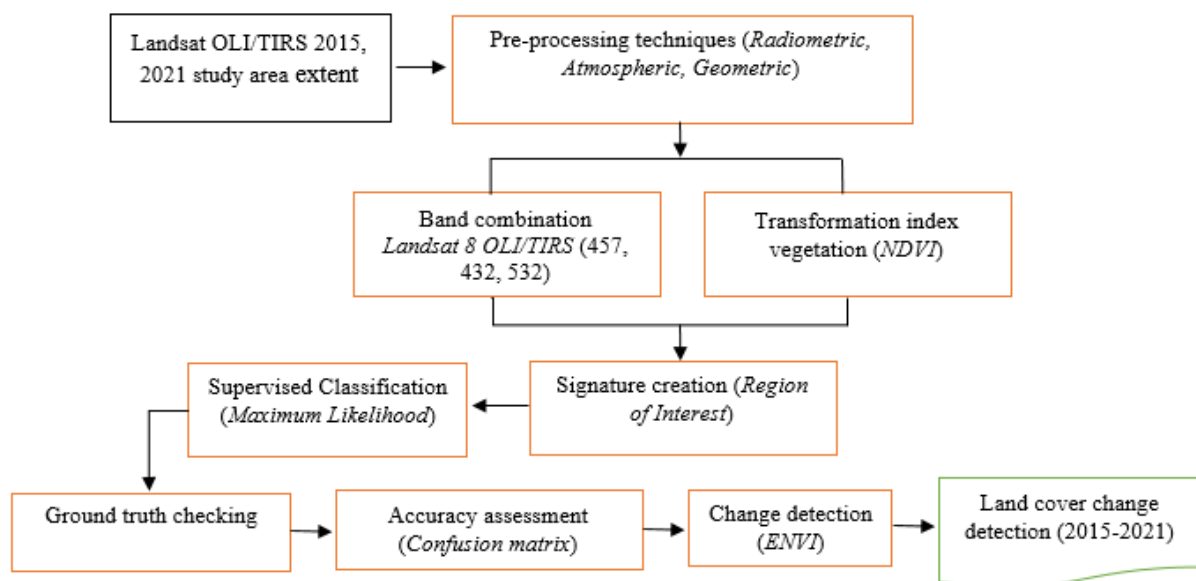


Figure 2. Research Flow Chart

## RESULTS AND DISCUSSION

### Preprocessing Image

Image data preprocessing consisted of geometric and radiometric corrections. The purpose of geometric correction was to minimize geometric distortion of the image, while radiometric correction was to improve image quality so that the spectral values in the image would be unbiased and consistent with the actual object (Danoedoro et al., 2015). Both 2015 and 2021 Landsat 8 OLI/TIRS images were corrected using the semi-automatic classification preprocessing feature for Landsat images in the Quantum GIS software.

### Spectral Indices and Multispectral Classification

The NDVI vegetation index utilizes the red and near-infrared channels in the Landsat 8 OLI/TIRS imagery, and the resultant is a digital number value ranging between -1 and +1. Still, the positive value generally indicates soil and vegetation objects (Ghorbani & Ouri, 2012). NDVI was used to separate vegetated from non-vegetated areas, which would be the basis for the multispectral classification. The brighter the object's appearance in the image indicates the denser the vegetation in the area. The brightness contrast or closer to +1 will result from the combination of high reflectance on the near-infrared and low reflectance on the red bands. At the same time, non-vegetation areas such as bare land, water body, and snow will have a much lower NDVI value (Lillesand et al., 2015).

Land-cover classification of Landsat 8 OLI/TIRS imagery refers to SNI 7645-1:2014 for a mapping scale of 1:50,000. The land-cover types used in this study consist of dryland forests, shrubs, dry-field, bare land, built-up area, and lakes. Land-cover classification uses the maximum likelihood supervised classification method, which is common and proven the most accurate among other supervised classification methods (Patil et al., 2012).

In this classification process, taking samples from each land cover type in the image, called the region of interest (ROI), was necessary. This ROI will mark pixels on certain land cover types for multispectral classification. Before taking ROI, composite images use several combinations, namely 457, 432, and 532. This composite image aimed to visually highlight an object in the picture.

### Land-cover Conditions in 2015

Based on the results of the land-cover analysis of a combination of spectral transformation and multispectral classification, it was found that land-cover in the Batur catchment area in 2015 was dominated by a dry-field area that is 29,02%, and the smallest is a built-up area that is 2,93% of the total area of the study. Table 1 shows the location of land-cover types based on image analysis in 2015 and 2021. Figure 3 and 4 show their distribution.

Based on the analysis of Landsat 8 OLI/TIRS imagery in 2015 and 2021, the total area of the research area is 10.184,85 ha or 101,84 km<sup>2</sup>. The details of land-cover types from largest to smallest are dry-field 2.955,53 ha or 29,02% of the research site area, dryland forest 2.346,3 ha or 23,04%, bare land 1,618.29 ha or 15,89%, lakes 1.547,34 ha or 15,19%, shrubs 1.422,3 ha or 13,94%, and built-up area 298,09 ha or 2,93%.

Sub-catchment with the built-up type land-cover area from the largest to smallest in 2015 were sub-catchment Melilit, with an area of 118,53 ha or 3,09% of the total sub-catchment area, followed by sub-catchment Kedisan with an area 63,79 ha or 8,95%, sub-catchment Blingkang with an area of 59,49 ha or 3,18%, sub-catchment Serongga with an area of 44,69 ha or 7,26%, then sub-catchment Gede Tampuriang and sub-catchment Trunyan with each of site 12,05 ha or 0,95%, and 10,84 ha or 3,44% of the total area of the sub-catchment.

Melilit and Blingkang sub-catchments were the two largest in the Batur catchment, with the widest dry field of 1,110.89 ha and 1,073.49 ha, respectively. The vast dry field

attracted the people, who were mostly farmers, to live there. However, the sub-catchments with the most densely populated areas were the Kedisan sub-catchments and Serongga sub-catchments. Kedisan sub-catchment includes several villages with a fairly large population, namely Kedisan, Buah, Abang Batudinding, and Abangsongan towns, with a population of 1,134 to 2,335 people (BPS, 2015). This sub-catchment also had many tourist support facilities in the form of lodging, hotels, and villas. In the Serongga sub-catchment, there is a village named Songan B, the most populous in Kintamani District, with 8,825 people living there (BPS, 2015). This population was high compared to other towns, where most were below that number.

Other sub-catchments that are Gede Tampuriang and Trunyan sub-catchments were two sub-catchments with a relatively small built-up area. The bare-land cover dominated the Gede Tampuriang sub-catchment, 675,62 ha or 53,66%. Most of this bare land was solid lava resulting from the eruption of Mount Batur, which was the Batur Geopark area, and the utilization was very limited. In contrast to the Trunyan sub-catchment, which is a sub-catchment dominated by the dry-land-forest cover, covering an area of 202,42 ha or 64,22% of the sub-catchment area, most of this sub-catchment area was an area with steep to very steep slopes, so it was not designated as a place of residence.

The sub-catchments with the largest shrubs area were Melilit, Gede Tampuriang, and Blingkang sub-catchments with 681,78 ha or 17,79%, 273,41 ha or 21,71% and 212,8 ha or 11,38% of the sub-catchment area. Based on the analysis results, the condition of shrubs is associated with dryland forest conditions, dry-field, and bare land. This is indicated by the sub-catchment, which has the largest area of shrubs and dryland forest, dry-field, and bare-land.

### **Land-cover Condition in 2021**

The types of land cover predominant in 2021 were dry-field with an area of

24,79%, and the smallest was a built-up area with 5,93% of the research area. Furthermore, in 2021 the details of land-cover area from largest to smallest are dry-field 2.525,11 ha or 24,79% of the research site area, bare land 2.070,54 ha or 20,33%, dryland forest 1.740,01 ha or 17,08%, shrubs 1.635,02 ha or 16,05%, lakes 1.610,07 ha or 15,81%, and built-up area 604,1 ha or 5,93%.

The sub-catchments with the largest to the smallest built-up land cover in 2021 include Melilit, Gede Tampuriang, Blingkang, Kedisan, Serongga, and Trunyan sub-catchments, with each covering 240.81 ha or 6,28%, 99,86 ha or 7,93%, 77,13 ha or 4,13%, 76,03 ha or 10,67%, 74,67 ha or 12,13% and 25,38 ha or 8,05% of the sub-catchment area.

Melilit and Blingkang sub-catchments are the two largest in the Batur catchment area, with the largest dry-field site covering 944,56 ha or 24,64% and 932,03 ha or 49,85% of the sub-catchment area. The existence of a large dry field attracts people who are mostly farmers to live in these two areas. This encourages the development of tourism activities in another sub-catchment, the Gede Tampuriang sub-catchment, where hot spring tourism is featured. At several points in this sub-catchment, effects occurred for supporting facilities such as minimarkets, inns, and villas. Furthermore, many facilities have been built to support local community activities in Kedisan and Serongga sub-catchments, which are densely populated.

Meanwhile, the Trunyan sub-catchment has a relatively small built-up area. This sub-catchment is dominated by dryland forest cover covering an area of 192,61 ha or 61,11% of its area. In addition, parts of the Trunyan sub-catchment have steep slopes, so it is unsuitable for residence.

The widest bare-land area is in the Melilit sub-catchment area, which is 1,108.87 ha or 28,93% of the sub-catchment area, and the smallest is in the Trunyan sub-catchment area, which is 11,12 ha or 3,53% of the sub-catchment area. Part of the Melilit sub-catchment area is used as a C-excavation sand mine, so some regions are bare without

vegetation. Mining activities that are still active have partially eroded other types of land cover, turning them into mining sites, especially in areas where the sand has not been utilized.

The sub-catchments with the largest shrubs area are the Melilit, Gede Tampuriang, and Blingkrank sub-catchments

with 814,39 ha or 21,25%, 320,86 ha or 25,48% and 241,96 ha or 12,94% of their area. Similar to 2015, shrubs type land cover condition is associated with dryland forest, dry-field, and bare-land. This can be seen in the sub-catchment, which has the largest area of shrubs and dryland forest, dry-field, and bare-land.

Table 1. Land cover in the Batur Catchment area based on Landsat 8 OLI/TIRS Image in 2015

No	Land-Cover Type	Land-Cover Area (ha)		Land-Cover Area (%)	
		2015	2021	2015	2021
1	Built-up Area	298,09	604,1	2,93	5,93
2	Dry field	2.955,53	2.525,11	29,01	24,79
3	Bare Land	1.618,29	2.070,54	15,88	20,32
4	Shrubs	1.422,3	1.638,02	13,96	16,08
5	Dryland Forest	2.436,3	1.740,01	23,03	17,08
6	Lake	1.547,34	1.610,07	15,19	15,80
7	Total	10.184,85	10.184,85	100	100

(Source: Image Analysis, 2021).

Table 2. Matrix of Land-cover Change in The Batur Catchment area Based on Landsat 8 OLI/TIRS Image 2015-2021 in Hectares

LC Type 2015	LC Type 2021							
	Bu	Df	Bl	Sh	Dlf	Lk	Total t1	Loses
Bu	151,5	91,12	18	0	21,81	15,66	298,09	146,59
Df	254,96	1.953,63	637,47	0	107,22	2,25	2.955,53	1001,9
Bl	78,12	36,18	1.359,45	139,95	3,15	1,44	1.618,29	258,84
Sh	75,33	286,14	50,22	856,36	149,81	1,44	1.419,3	562,94
Dlf	38,88	158,04	4,68	638,53	1.456,58	49,59	2.346,3	889,72
Lk	5,31	0	0,72	0,18	1,44	1.539,69	1.547,34	7,65
Total t2	604,1	2.525,11	2.070,54	1.635,02	1.740,01	1.610,07	10.184,85	
Gain	452,6	571,48	711,09	778,66	283,43	70,38		
Net change	306,01	-430,42	452,25	215,72	-606,29	62,73		

(Source: Image Analysis, 2021).

Information

LC = Land-cover

Bu= Build-up area

Sh = shrubs

Bl = Bare land

Df = Dry field

Dlf = Dryland Forest

Lk = Lake

Table 3. Land-cover in the Sub Catchment area Batur Based on Landsat 8 OLI/TIRS Image in 2015

Sub Catchment area	Land-Cover Type											
	Bu		Df		Bl		Sh		Dlf		Lk	
	2015	2021	2015	2021	2015	2021	2015	2021	2015	2021	2015	2021
Blingkang	59,49	77,13	1.073,49	932,03	2,76	250,03	212,8	241,96	520,93	367,42	0,02	0,92
Gede Tampuriang	12,05	99,86	141,3	116,72	675,62	595,73	273,41	320,86	156,75	124,22	0,04	1,78
Kedisan	63,79	76,03	211,84	127,39	4,11	63,69	64,53	156,81	359,48	279,3	9,12	9,65
Melilit	118,53	240,81	1.110,89	944,56	904,83	1.108,87	681,78	814,39	1.016,88	724,28	0	0
Serongga	44,69	74,67	376,92	394,16	28,61	39,14	124,05	57,72	41,46	49,41	0	0,63
Trunyan	10,84	25,38	29,52	7,07	0,75	11,12	57,49	69,21	202,42	192,61	14,17	9,8
Amount	309,39	593,88	2.943,96	2.521,93	1.616,68	2.068,58	1.414,06	1661	2.297,92	1.737,2	23,35	22,78

(Source: Image Analysis, 2021).

Information

LC = Land-cover

Bu= Build-up area

Sh = shrubs

Bl = Bare land

Df = Dry field

Dlf = Dryland Forest

Lk = Lake

Accuracy Assessment of Multispectral Classification

The accuracy assessment used the confusion matrix calculation method (Russell G. Congalton, 2019), providing producer, user, and overall accuracy. The Kappa coefficient was not recommended for accuracy assessment, so the value of the kappa coefficient was not included (Foody, 2020; Pontius & Millones, 2011). When mapped, the standard of the overall accuracy of land-cover classification is already determined, which is at least 85% (Giri, 2012).

Land-cover data from the multispectral classification of Landsat 8 OLI/TIRS images in 2015 was tested using QuickBird images recorded in 2015, while land-cover data in 2021 was tested using field data and interviews in 2021. The accuracy of maps generated from remote sensing techniques is affected by

several factors, including site-specific characteristics (Hsiao & Cheng, 2016; Millard & Richardson, 2015), choice of data classifier (Heydari & Mountrakis, 2018; Khatami et al., 2016), and selection of training data for classification (Hsiao & Cheng, 2016; Shao & Lunetta, 2012). Integrating earth observation and other data from multiple sources is required to derive information with sufficient accuracy and detail over large areas (Herold et al., 2016).

The comparison of the accuracy of land-cover classification is shown in Table 4. The overall accuracy test in 2015 was 82,63%, while in 2021, the result of the accuracy assessment was 89,57%. This shows that maximum likelihood classification is more realistic than random classification (Tadele et al., 2017).

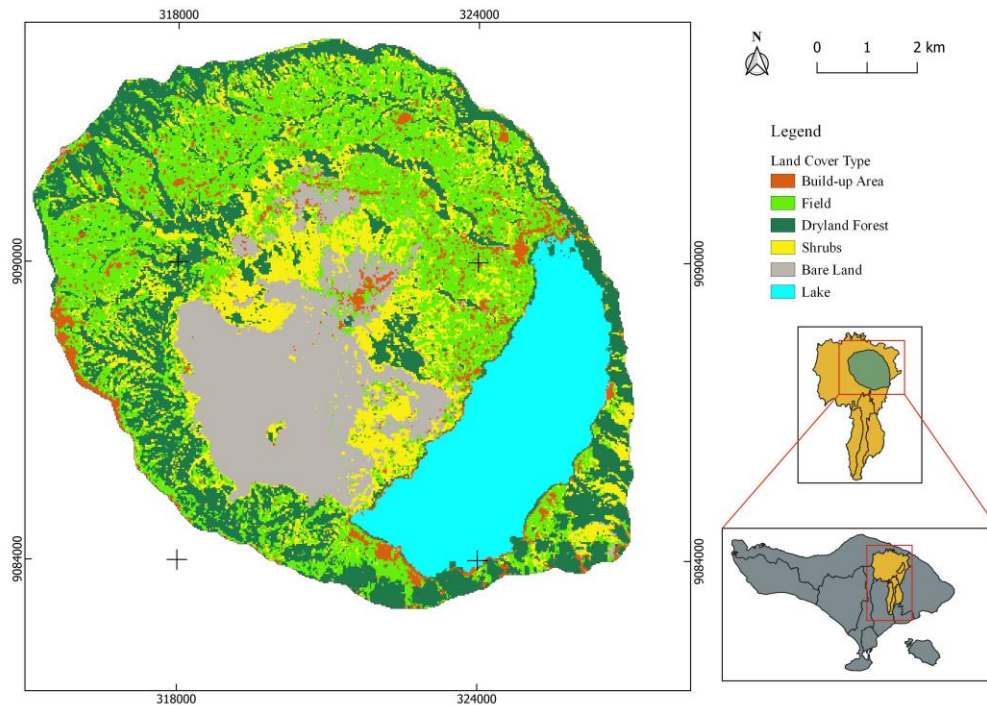


Figure 3. Land-cover Map Batur Catchment area in 2015 (Source: Image Analysis, 2021)

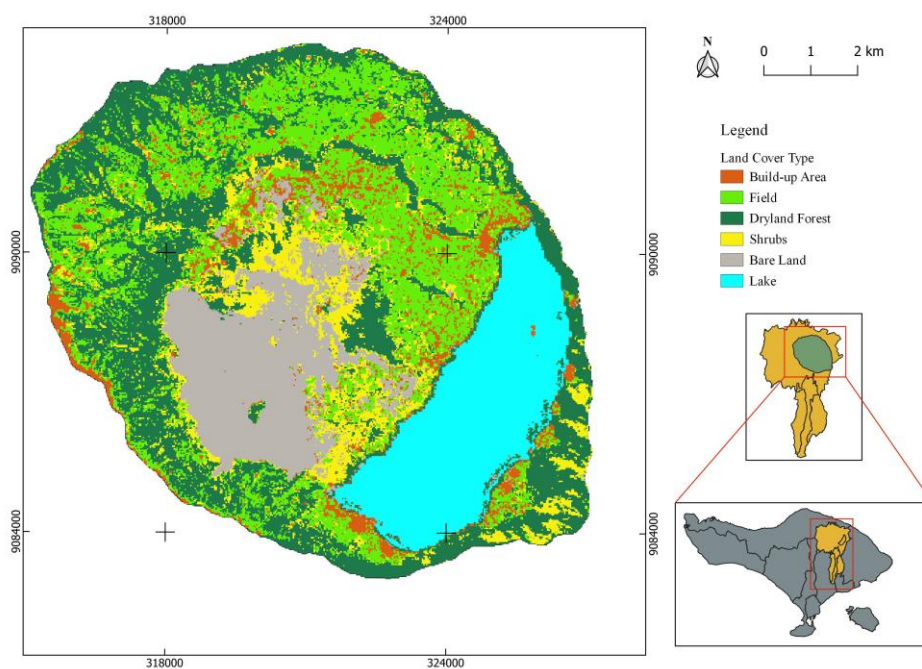


Figure 4. Land-cover Map Batur Catchment area in 2021 (Source: Image Analysis, 2021)

The accuracy value in 2015 is lower than in 2021, and this is because some of the research areas in the 2015 Landsat 8 OLI/TIRS imagery were covered with clouds, causing misclassification, in contrast to the Landsat 8 OLI/TIRS image data in 2021, which was free from cloud disturbances. However, based on the overall accuracy value, the land-cover class

in 2015 does not meet the minimum standard for land-cover class classification, while the land-cover class in 2021 meets the minimum standard for the land-cover category. Cloud-covered area of 2015 Landsat OLI/TIRS imagery could increase the error value in the classification results (Zylshal et al., 2016) and making less accurate the interpretation

(Danoedoro et al., 2020), which resulting lower accuracy.

The difference in time between image recording and the accuracy of sampling in the field affects the planting period of seasonal plants in the Batur catchment area. Some locations were dry-field during image

recording but bare-land during selection because they had not been planted. This difference affects the classification results and the level of accuracy associated with the spectral differences reflected by objects before and after harvesting (Lu et al., 2016).

Table 4. Comparison of Accuracy Parameters Landc-cover Classification in 2015-2021

LC Classification	2015					2021				
	PA	UC	C	O	OA	PA	UC	C	O	OA
Bu	63,16	73,28	26,72	36,84		84,21	72,43	28,57	15,79	
Df	71,64	72,24	27,76	23,39		83,61	84,3	15,7	16,39	
Bl	92,16	94,84	5,16	7,84	82,63%	85,83	92,79	7,21	14,17	89,57%
Sh	74,36	38,16	61,84	25,64		77,08	97,37	2,63	22,92	
Dlf	76,92	81,74	18,26	28,36		100	96,34	3,66	0	
Lk	93,59	99,69	0,31	6,41		100	100	0	0	

(Source: Image Analysis, 2021).

Information

PA = Produser accuracy

UC= User accuracy

C = Commission

O = Omission

OA= Overall accuracy

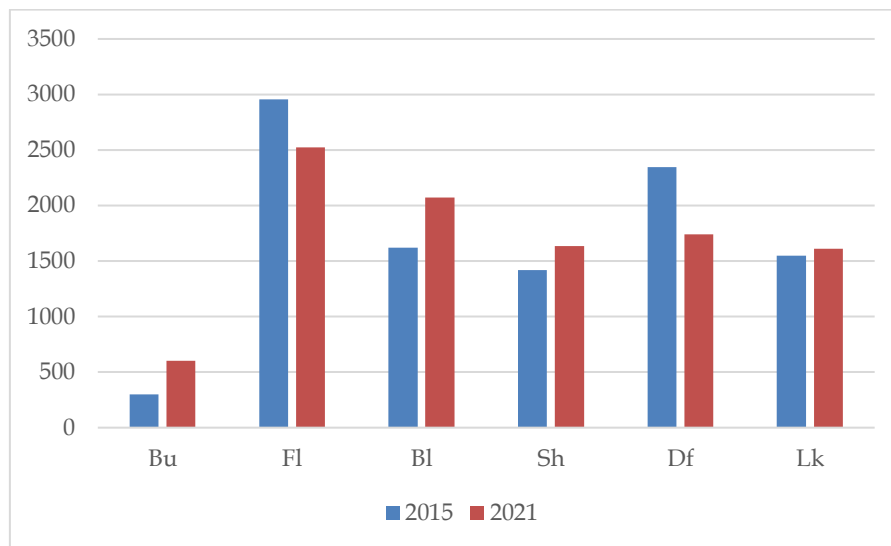


Figure 5. Land-cover Change Chart Batur Catchment area in 2015-2021

(Source: Image Analysis, 2021).

Identification of Land-cover Change

Identification of land cover spatial changes uses the change detection feature in ENVI 4.5 software. This feature is a change detection method that compares post-

classification spectral data. The change detection method using spectral data is considered capable of producing higher accuracy than change detection using patterns (Viana et al., 2019; He et al., 2019).

In this study, the authors focused specifically on the types of land cover changes that occurred.

Based on the results of the crosstabulation in Table 3 and Figure 5, four types of land cover have increased the area from 2015-2021, which are bare land by 452,25 ha or an increase of 27,95% from the previous area, built-up land by 306.01 ha or 102,66 %, shrubs by 215,72 ha or 15,20% and lakes 62,73 ha or an increase of 4,05% from the previous area. Furthermore, other types of land cover have decreased in the area. Namely, dryland forest decreased by -606,29 ha or -25,84% of the prior area and dry field by -430.42 ha or 14,56% of the previous area. When viewed in terms of proportions in Table 3, in 2015, the type of land cover was dominated by dry-field with an area of 29,02%, followed by dryland forest at 23,04%, bare-land 15,89%, the lake at 15,19%, shrubs at 13,94%, and 2,93% built-up land. Similarly, in 2021 the type of land cover is still dominated by dry-field with an area of 24,79%, followed by bare-land 20,33%, dryland forest at 17,08%, shrubs at 16,05%, lakes at 15,81%, and built-up land at 5,93%. Based on this description, the proportion of dryland forest decreased by -5,95% and dry-field by 4,23%, while bare-land increased by 4,44%, shrubs by 2,12% and built-up land increased by 3% and lakes increased by 0,62 %.

Tables 2 and 3 show that there is a change in land cover in the Batur catchment for a period of six years from 2015 to 2021. The increase in the area occurred in the types of built-up land cover, bare land, shrubs, and lakes. Meanwhile, dry-field and forests tend to decrease in area.

Built-up land-cover type is increasing throughout the Batur catchment area. The biggest change was in the Melilit sub-catchment, which increased by 122,28 ha from the previous area, while the lowest was in the Kedisan sub-catchment, which was 12,12 ha. Furthermore, dry field decreased

for most of the area; the highest was in the Melilit sub-catchment, which fell by -166.33 ha, and the lowest was in Trunyan sub-catchment by -22,45 ha. However, the dry-field area has increased in the Serongga sub-catchment area, supplemented by 17,24 ha from the previous area.

Most of the bare-land area has increased, the highest is in the Blingkang sub-catchment at 247,27 ha, and the lowest is in the Trunyan sub-catchment at 10,37 ha. However, bare land in the Gede Tampuriang sub-catchment decreased by -79,89 ha. Like bare-land, most of the shrubs area has increased; the highest is in the Melilit sub-catchment of 204,04 ha, and the lowest is in the Trunyan sub-catchment with 11,72 ha, but the area of Serongga sub-catchment is decreased by -66,33 ha. Finally, the dryland forest with the highest reduction in area is in Melilit Sub-catchment at -292,6 ha, and the lowest is in Trunyan Sub-catchment at -9,81 ha. However, in the Serongga sub-catchment, the area of dryland forest is increased by 7,95 ha.

Tables 1 and 2 show the phenomenon of a spurious change, for example, changes in land cover that are built up into dry dry-field or built-up areas into forests. This is very difficult to happen, so changes in the ostensibly could cause it. Different images with two other recording times generally have other atmospheric conditions, including sun angles, height, and off-nadir distance, resulting in different illumination levels. This difference will produce changes as if the data were classified (Zhu et al., 2021). Furthermore, (Sood et al., 2021) convey that changes occur due to slope variability, topographic roughness, and topographic effects (shadows).

Differences in rainfall also play an essential role in detecting land cover changes. The rainfall in the 2015 recorded image in May was 36-44 mm, while the rain in May-June in 2021 ranged from 0-33 mm (BMKG, 2021). This difference in rainfall results in humidity, which causes a spurious change (Zhu et al., 2021). Different humidity in the rainy and dry seasons results in significant differences in soil

moisture. It changes the location of shorelines, lakes, and rivers (Zhu et al., 2021), showing differences in visual appearance in these areas. In addition to several factors described previously, the changes seem to be caused by differences in the spectrum on cultivated land before and after harvest (Lu et al., 2016), disturbances from pests and diseases on cultivated plants and forests (Ren et al., 2012) and water turbidity (Chen et al., 2013).

## CONCLUSION

Based on the results of the research, we concluded that there were changes in land-cover types in the Batur Catchment area, including an increase of bare land cover by 452.25 ha (27,95%), built-up area by 306.01 ha (102,66%), shrubs by 215,72 ha (15,20%), and the lake area by 62.73 ha (4,50%). Furthermore, dry-field area and dryland forest decreased by -430,42 ha (-14,56%) and -606,29 ha (25,84%). Land-cover change occurs in all sub-DATA areas of varying sizes.

The land-cover classification accuracy assessment of Landsat OLI/TIRS images using the maximum likelihood method in 2015 showed an accuracy rate is 82,63%, while in 2021, the accuracy rate was 89,59%. Cloud disturbances in 2015 image data greatly affected land-cover classification accuracy for that year, as seen from the lower accuracy rate compared to 2021.

## ACKNOWLEDGMENT

The author would like to thank Lembaga Pengelola Dana Pendidikan (LPDP) of the Ministry of Finance of the Republic of Indonesia for supporting scholarships and research funding. The author also expresses her gratitude to the final project supervisor and the academic community of the Master of Remote Sensing Study Program, Faculty of Geography, Gadjah Mada University.

## REFERENCE LIST

Abdullah, A. Y. M., Masrur, A., Gani Adnan, M. S., Al Baky, M. A., Hassan, Q. K., & Dewan, A. (2019). Spatio-temporal patterns of land use/land cover

change in the heterogeneous coastal region of Bangladesh between 1990 and 2017. *Remote Sensing*, 11(7). <https://doi.org/10.3390/rs11070790>

Adebayo, H. O., Otun, W. O., & Daniel, I. S. (2019). Change Detection in Landuse/Landcover of Abeokuta Metropolitan Area, Nigeria Using Multi-Temporal Landsat Remote Sensing. *Indonesian Journal of Geography*, 51(2), 217–223.

Alam, S. M. R., & Hossain, M. S. (2020). A Rule-Based Classification Method for Mapping Saltmarsh Land-Cover in South-Eastern Bangladesh from Landsat-8 OLI. *Canadian Journal of Remote Sensing*, 1–25. <https://doi.org/10.1080/07038992.2020.1789852>

Alkaradaghi, K., Ali, S. S., Al-Ansari, N., & Laue, J. (2018). Evaluation of Land Use & Land Cover Change Using Multi-Temporal Landsat Imagery: A Case Study Sulaimaniyah Governorate, Iraq. *Journal of Geographic Information System*, 10(03), 247–260. <https://doi.org/10.4236/jgis.2018.103013>

Aslami, F., & Ghorbani, A. (2018). Object-based land-use/land-cover change detection using Landsat imagery: a case study of Ardabil, Namin, and Nir counties in northwest Iran. *Environmental Monitoring and Assessment*, 190(7). <https://doi.org/10.1007/s10661-018-6751-y>

Barakat, A., Ouargaf, Z., Khellouk, R., El Jazouli, A., & Touhami, F. (2019). Land Use/Land Cover Change and Environmental Impact Assessment in Béni-Mellal District (Morocco) Using Remote Sensing and GIS. *Earth Systems and Environment*, 3(1), 113–125. <https://doi.org/10.1007/s41748-019-00088-y>

Bektas Balcik, F., & Karakacan Kuzucu, A. (2016). Determination of land cover/land use using spot 7 data with supervised classification methods.

- International Archives of the Photogrammetry, Remote Sensing and Spatial Information Sciences - ISPRS Archives, 42(2W1), 143-146. <https://doi.org/10.5194/isprs-archives-XLII-2-W1-143-2016>
- Berihun, M. L., Tsunekawa, A., Haregeweyn, N., Meshesha, D. T., Adgo, E., Tsubo, M., Masunaga, T., Fenta, A. A., Sultan, D., Yibeltal, M., & Ebabu, K. (2019). Hydrological responses to land use/land cover change and climate variability in contrasting agroecological environments of the Upper Blue Nile basin, Ethiopia. *Science of the Total Environment*, 689, 347-365. <https://doi.org/10.1016/j.scitotenv.2019.06.338>
- Campbell, J.B., & Wynne, R. . (2011). *Introduction to remote sensing*. Guilford Press.
- Chen, J., Lu, M., Chen, X., Chen, J., & Chen, L. (2013). A spectral gradient difference-based approach for land cover change detection. *ISPRS Journal of Photogrammetry and Remote Sensing*, 85, 1-12. <https://doi.org/10.1016/j.isprsjprs.2013.07.009>
- Danoedoro, Projo., Kristian, Gerry., Rahmi, K. N. . (2015). Pengaruh Metode Koreksi Radiometrik ALOS AVNIS-2 Terhadap Akurasi Hasil Estimasi Karbon Vegetasi Tegakan di Wilayah Kota Semarang Bagian Timur. *Prosiding PIT MAPIN XX*.
- Danoedoro, P., Ananda, I. N., Kartika, C. S. D., Umela, A. F., & Alvidita. (2020). Testing a detailed classification scheme for land-cover/ land-use mapping of typical Indonesian landscapes: Case study of Sorolangun, Jambi, and Salatiga, Central Java. *Indonesian Journal of Geography*, 52(3), 327-340.
- Footy, G. M. (2020). Explaining the unsuitability of the kappa coefficient in the assessment and comparison of the accuracy of thematic maps obtained by image classification. *Remote Sensing of Environment*, 239. <https://doi.org/10.1016/j.rse.2019.111630>
- Garg, V., Nikam, B. R., Thakur, P. K., Aggarwal, S. P., Gupta, P. K., & Srivastav, S. K. (2019). Human-induced land use land cover change and its impact on hydrology. *HydroResearch*, 1, 48-56. <https://doi.org/10.1016/j.hydres.2019.06.001>
- Ghorbani, A., & Ouri, A. E. (2012). Utility of the NDVI for land/canopy cover mapping in Khalkhal County (Iran). *Annals of Biological Research*, 3(12), 5494-5503. <https://www.researchgate.net/publication/284777424>
- Giri, C. P. (2012). *Remote Sensing of Land Use and Land Cover: Principles and Applications (Vol. 1)*.
- Herold, M., See, L., Tsensbazar, N. E., & Fritz, S. (2016). Towards an integrated global land cover monitoring and mapping system. *Remote Sensing*, 8(12), 1-11. <https://doi.org/10.3390/rs8121036>
- Heydari, S. S., & Mountrakis, G. (2018). Effect of classifier selection, reference sample size, reference class distribution and scene heterogeneity in per-pixel classification accuracy using 26 Landsat sites. *Remote Sensing of Environment*, 204, 648-658. <https://doi.org/10.1016/j.rse.2017.09.035>
- Hsiao, L. H., & Cheng, K. S. (2016). Assessing uncertainty in LULC classification accuracy by using bootstrap resampling. *Remote Sensing*, 8(9). <https://doi.org/10.3390/rs8090705>
- Hua, W., Chen, H., Sun, S., & Zhou, L. (2015). Assessing climatic impacts of future land use and land cover change projected with the CanESM2 model. *International Journal of Climatology*, 35(12), 3661-3675. <https://doi.org/10.1002/joc.4240>
- Jazouli, A. El, Barakat, A., Khellouk, R., Rais, J., & Baghdadi, M. El. (2019). Remote sensing and GIS techniques for

- prediction of land use land cover change effects on soil erosion in the high basin of the Oum Er Rbia River (Morocco). *Remote Sensing Applications: Society and Environment*, 13, 361–374. <https://doi.org/10.1016/j.rsase.2018.12.004>
- Ji, D. R. H. Y. W. F. B. Z. Q. (2012). Crop diseases and pests monitoring based on remote sensing: A survey. *World Automation Congress 2012, Puerto Vallarta, Mexico*, 177–181.
- Kementerian Lingkungana Hidup (KLH). (2014). *Gerakan Penyelamatan Danau (GERMADAN) Danau Batur*.
- Khatami, R., Mountrakis, G., & Stehman, S. V. (2016). A meta-analysis of remote sensing research on supervised pixel-based land-cover image classification processes: General guidelines for practitioners and future research. *Remote Sensing of Environment*, 177, 89–100. <https://doi.org/10.1016/j.rse.2016.02.028>
- Letsoin, S. M. A., Herak, D., Rahmawan, F., & Purwestri, R. C. (2020). Land cover changes from 1990 to 2019 in Papua, Indonesia: Results of the remote sensing imagery. *Sustainability (Switzerland)*, 12(16), 1–18. <https://doi.org/10.3390/su12166623>
- Lin, L., Hao, Z., Post, C. J., Mikhailova, E. A., Yu, K., Yang, L., & Liu, J. (2020). Monitoring land cover change on a rapidly urbanizing island using google earth engine. *Applied Sciences (Switzerland)*, 10(20), 1–16. <https://doi.org/10.3390/app10207336>
- Lu, M., Chen, J., Tang, H., Rao, Y., Yang, P., & Wu, W. (2016). Land cover change detection by integrating object-based data blending model of Landsat and MODIS. *Remote Sensing of Environment*, 184, 374–386. <https://doi.org/10.1016/j.rse.2016.07.028>
- Millard, K., & Richardson, M. (2015). On the importance of training data sample selection in Random Forest image classification: A case study in peatland ecosystem mapping. *Remote Sensing*, 7(7), 8489–8515. <https://doi.org/10.3390/rs70708489>
- Mohamed, M. A., Anders, J., & Schneider, C. (2020). Monitoring of changes in land use/land cover in Syria from 2010 to 2018 using multitemporal Landsat imagery and GIS. *Land*, 9(7). <https://doi.org/10.3390/land9070226>
- Mohammadi, A., Shahabi, H., & Ahmad, B. Bin. (2019). Land-cover change detection in a part of Cameron highlands, Malaysia using ETM+ satellite imagery and support vector machine (SVM) algorithm. *EnvironmentAsia*, 12(2), 145–154. <https://doi.org/10.14456/ea.2019.36>
- Moser, G., Serpico, S. B., & Benediktsson, J. A. (2013). Land-cover mapping by Markov modeling of spatial-contextual information in very-high-resolution remote sensing images. *Proceedings of the IEEE*, 101(3), 631–651. <https://doi.org/10.1109/JPROC.2012.2211551>
- Mukherjee, F., & Singh, D. (2020). Assessing Land Use–Land Cover Change and Its Impact on Land Surface Temperature Using LANDSAT Data: A Comparison of Two Urban Areas in India. *Earth Systems and Environment*, 4(2), 385–407. <https://doi.org/10.1007/s41748-020-00155-9>
- P3E Bali Nusra. (2018). *Rencana Pengelolaan Sumber Daya Air Dan Lahan Di Danau Batur Serta Daerah Tangkapan Airnya Berbasis Daya Dukung Lingkungan Hidup*. November.
- Patil, M. B., Desai, C. G., & Umrikar, B. N. (2012). Image Classification Tool for Land Use / Land Cover Analysis: a Comparative Study of Maximum Likelihood and Minimum Distance Method. *International Journal of Geology, Earth, and Environmental Sciences*, 2(3), 189–196.

- <http://www.cibtech.org/jgee.htm>
- Patil, R. J. (2018). Spatial Techniques for Soil Erosion Estimation. [https://doi.org/10.1007/978-3-319-74286-1\\_4](https://doi.org/10.1007/978-3-319-74286-1_4)
- Phiri, D., Morgenroth, J., Xu, C., & Hermosilla, T. (2018). Effects of preprocessing methods on Landsat OLI-8 land cover classification using OBIA and random forests classifier. *International Journal of Applied Earth Observation and Geoinformation*, 73, 170–178. <https://doi.org/10.1016/j.jag.2018.06.014>
- Pontius, R. G., & Millones, M. (2011). Death to Kappa: Birth of quantity disagreement and allocation disagreement for accuracy assessment. *International Journal of Remote Sensing*, 32(15), 4407–4429. <https://doi.org/10.1080/01431161.2011.552923>
- Potapov, P., Hansen, M. C., Kommareddy, I., Kommareddy, A., Turubanova, S., Pickens, A., Adusei, B., Tyukavina, A., & Ying, Q. (2020). Landsat analysis ready data for global land cover and land cover change mapping. *Remote Sensing*, 12(3). <https://doi.org/10.3390/rs12030426>
- Rahman, A., Kumar, S., Fazal, S., & Siddiqui, M. A. (2012). Assessment of Land use/land cover Change in the Northwest District of Delhi Using Remote Sensing and GIS Techniques. *Journal of the Indian Society of Remote Sensing*, 40(4), 689–697. <https://doi.org/10.1007/s12524-011-0165-4>
- Rathnayake, C. W. M., Jones, S., & Soto-Berelov, M. (2020). Mapping land cover change over a 25-year period (1993-2018) in Sri Lanka using Landsat time-series. *Land*, 9(1). <https://doi.org/10.3390/land9010027>
- Rawat, J. S., & Kumar, M. (2015). Monitoring land use/cover change using remote sensing and GIS techniques: A case study of Hawalbagh block, district Almora, Uttarakhand, India. *Egyptian Journal of Remote Sensing and Space Science*, 18(1), 77–84. <https://doi.org/10.1016/j.ejrs.2015.02.002>
- Russell G. Congalton, K. G. (2019). *Assessing the Accuracy of Remotely Sensed Data*. CRC Press.
- Rwanga, S. S., & Ndambuki, J. M. (2017). Accuracy Assessment of Land Use/Land Cover Classification Using Remote Sensing and GIS. *International Journal of Geosciences*, 08(04), 611–622. <https://doi.org/10.4236/ijg.2017.84033>
- Shao, Y., & Lunetta, R. S. (2012). Comparison of support vector machine, neural network, and CART algorithms for the land-cover classification using limited training data points. *ISPRS Journal of Photogrammetry and Remote Sensing*, 70, 78–87. <https://doi.org/10.1016/j.isprsjprs.2012.04.001>
- Sharma, A., Liu, X., Yang, X., & Shi, D. (2017). A patch-based convolutional neural network for remote sensing image classification. *Neural Networks*, 95, 19–28. <https://doi.org/10.1016/j.neunet.2017.07.017>
- Sood, V., Gusain, H. S., Gupta, S., & Singh, S. (2021). Topographically derived subpixel-based change detection for monitoring changes over rugged terrain Himalayas using AWiFS data. *Journal of Mountain Science*, 18(1), 126–140. <https://doi.org/10.1007/s11629-020-6151-y>
- Sun, C., Fagherazzi, S., & Liu, Y. (2018). Classification mapping of salt marsh vegetation by flexible monthly NDVI time-series using Landsat imagery. *Estuarine, Coastal and Shelf Science*, 213, 61–80. <https://doi.org/10.1016/j.ecss.2018.08.007>
- Stasiun Klimatologi Jembrana. (2012). *Badan Meteorologi Klimatologi dan Geofisika (BMKG). Informasi Hujan*

- Sy, S., & Quesada, B. (2020). Anthropogenic land cover change impact on climate extremes during the 21st century. *Environmental Research Letters*, 15(3). <https://doi.org/10.1088/1748-9326/ab702c>
- Taati, A., Sarmadian, F., & Mousavi, A. (2016). Land Use Classification using Support Vector Machine and Maximum Likelihood Algorithms by Landsat 5 TM Images. *Walailak Journal*, 12(8), 681-687. <https://doi.org/10.14456/WJST.2015.33>
- Tadele, H., Mekuriaw, A., Selassie, Y. G., & Tsegaye, L. (2017). Land Use/Land Cover Factor Values and Accuracy Assessment Using a GIS and Remote Sensing in the Case of the Quashay Watershed in Northwestern Ethiopia. *Journal of Natural Resources and Development*, 38-44. <https://doi.org/10.5027/jnrd.v7i0.05>
- Thomas M. Lillesand, Ralph W. Kiefer, J. W. C. (2015). *Remote Sensing and Image Interpretation* (Seventh Ed). WILEY.
- Thyagarajan, K. K., & Vignesh, T. (2019). Soft Computing Techniques for Land Use and Land Cover Monitoring with Multispectral Remote Sensing Images: A Review. *Archives of Computational Methods in Engineering*, 26(2), 275-301. <https://doi.org/10.1007/s11831-017-9239-y>
- Vinayak, B., Lee, H. S., & Gedem, S. (2021). Prediction of land use and land cover changes in Mumbai city, India, using remote sensing data and a multilayer perceptron neural network-based Markov Chain model. *Sustainability (Switzerland)*, 13(2), 1-22. <https://doi.org/10.3390/su13020471>
- Weih, R. C., & Riggan, N. D. (2010). The International Archives of the Photogrammetry. In *Remote Sensing and Spatial Information Sciences*.
- Wu, K., Du, Q., Wang, Y., & Yang, Y. (2017). Supervised sub-pixel mapping for change detection from remotely sensed images with different resolutions. *Remote Sensing*, 9(3). <https://doi.org/10.3390/rs9030284>
- Wulder, M. A., Loveland, T. R., Roy, D. P., Crawford, C. J., Masek, J. G., Woodcock, C. E., Allen, R. G., Anderson, M. C., Belward, A. S., Cohen, W. B., Dwyer, J., Erb, A., Gao, F., Griffiths, P., Helder, D., Hermosilla, T., Hipple, J. D., Hostert, P., Hughes, M. J., ... Zhu, Z. (2019). Current status of Landsat program, science, and applications. *Remote Sensing of Environment*, 225, 127-147. <https://doi.org/10.1016/j.rse.2019.02.015>
- Zhai, H., Lv, C., Liu, W., Yang, C., Fan, D., Wang, Z., & Guan, Q. (2021). Understanding Spatio-Temporal Patterns of Land Use / Land. *Remote Sensing, 2000-2019*.
- Zhu, L., Gao, D., Jia, T., & Zhang, J. (2021). Using Eco-geographical zoning data and crowdsourcing to improve the detection of spurious land cover changes. *Remote Sensing*, 13(16). <https://doi.org/10.3390/rs13163244>
- Zylshal, Z., Susanto, H., & Hidayat, S. (2016). Ekstraksi Informasi Penutup Lahan Area Luas Dengan Metode Expert Knowledge Object-Based Image Analysis (Obia) Pada Citra Landsat 8 OLI Pulau Kalimantan. *Majalah Ilmiah Globe*, 18(1), 09. <https://doi.org/10.24895/mig.2016.18-1.390>